
Spectral Image Segmentation with Global Appearance Modeling

Jeova F. S. Rocha Neto
School of Engineering
Brown University
Providence, RI 02906
jeova_farias@brown.edu

Pedro F. Felzenszwalb
School of Engineering
Brown University
Providence, RI 02906
pff@brown.edu

Abstract

We introduce a new spectral method for image segmentation that incorporates long range relationships for global appearance modeling. The approach combines two different graphs, one is a sparse graph that captures spatial relationships between nearby pixels and another is a dense graph that captures pairwise similarity between *all pairs of pixels*. We extend the spectral method for Normalized Cuts to this setting by combining the transition matrices of Markov chains associated with each graph. We also derive an efficient method that uses importance sampling for sparsifying the dense graph of appearance relationships. This leads to a practical algorithm for segmenting high-resolution images. The resulting method can segment challenging images without any filtering or pre-processing.

1 Introduction

Image segmentation is a fundamental problem in computer vision. Spectral clustering methods pioneered by the normalized cuts approach [1] provide simple and powerful algorithms based on fundamental graph-theoretic notions and computational linear algebra.

Spectral clustering methods are formulated using an objective function defined by a graph. The classical constructions used for image segmentation focus on pairwise similarity between nearby pixels. In this paper we introduce a new spectral method that incorporates long range relationships for global appearance modeling. The resulting method can segment challenging images without any filtering or pre-processing. Figure 1 shows several results obtained with the proposed method. Figure 2 shows how the new method significantly outperforms the original normalized cuts formulation.

We use a dense graph to capture the global appearance of regions. The normalized cut in this graph captures the distributions of pixel values in each region using a kernel density estimate. The measure penalizes the overlap between distributions in different regions.

To implement our image segmentation approach we extend the normalized cuts spectral algorithm to a setting where there are multiple graphs that encode different grouping cues. Our approach for image segmentation combines two graphs. We provide a natural interpretation for the normalized cut criteria on each of these graphs. One of the graphs is sparse and does not depend on the image data, it simply captures spatial relationships between pixels. The other graph is dense and captures pairwise similarity between *all pairs of pixels*.

The direct implementation of spectral methods to segment high resolution images is always difficult due to memory and computational requirements. We tackle this challenge using a graph sparsification approach that enables the efficient segmentation of high resolution images.



Figure 1: Segmentation results using the proposed method

We show experimental results with a variety of images and provide a quantitative evaluation using a dataset of synthetic images with Brodatz textures. Our approach achieves highly accurate results in this setting despite the complex appearance of the textures.

2 Background

2.1 Graph cuts and spectral clustering

Let $G = (V, E, w)$ be an undirected weighted graph. A cut (A, B) is a partition of V into two disjoint sets. We consider the weight of a cut in different graphs with the same set of vertices. Let $w(i, j) = 0$ when $\{i, j\} \notin E$. The weight of a cut (A, B) in G is defined as,

$$\text{Cut}(A, B|G) = \sum_{i \in A, j \in B} w(i, j). \quad (1)$$

In the context of clustering and image segmentation it is typical to use large weights to indicate that elements are similar and should be grouped together. In this case we can look for the *minimum cut* to find an optimal partition of V . However, this strategy is heavily biased towards imbalanced cuts, such as having a single node on one side. This motivated the introduction of the celebrated normalized cut criteria and algorithm [1].

The *normalized cut* value is defined as,

$$\text{NCut}(A, B|G) = \frac{\text{Cut}(A, B|G)}{\text{Vol}(A|G)} + \frac{\text{Cut}(A, B|G)}{\text{Vol}(B|G)} = \text{Vol}(V|G) \frac{\text{Cut}(A, B|G)}{\text{Vol}(A|G) \text{Vol}(B|G)}. \quad (2)$$

Here $\text{Vol}(A|G)$ is called the the volume of A and is defined as $\text{Vol}(A|G) = \sum_{i \in A, j \in V} w(i, j)$. The spectral algorithm introduced in [1] solves a continuous relaxation of the minimum NCut problem. Let W be the weighted adjacency matrix of G . Let D be the diagonal degree matrix with $D(i, i) = \sum_{j \in V} W(i, j)$. The matrix $L = D - W$ is the *Laplacian* of G .

The NCut algorithm solves a generalized eigenvector problem,

$$Lx = \lambda Dx. \quad (3)$$

The algorithm selects the eigenvector x with second smallest eigenvalue, and partitions V by thresholding x . In [2] the NCut criteria and algorithm is described in terms of a Markov chain. Let $P = D^{-1}W$. The matrix P is the transition matrix of a Markov chain over the vertices V . The long term behavior of this Markov chain can be characterized by the solutions to the eigenvector problem

$$Px = \lambda x. \quad (4)$$

A solution (λ, x) to the eigenvector problem in (4) leads to a solution $(1 - \lambda, x)$ to the generalized eigenvector problem in (3) and vice-versa. Therefore the generalized eigenvector x used in the NCut algorithm corresponds to the eigenvector of P with second largest eigenvalue.

2.2 Normalized Cuts for Image Segmentation

The classical application of normalized cuts for image segmentation involves a graph H where the vertices represent the image pixels and the weights reflect both the appearance similarity and distance between pairs pixels.

Let $H = (V, E, w)$ be a graph where the vertices V are the pixels in an image and the edges E connect every pair of pixels. We use $I(j)$ and $X(j)$ to denote respectively the appearance (such as the brightness or color) and spatial location of pixel j . Now define,

$$w(i, j) = \exp\left(-\frac{\|I(i) - I(j)\|^2}{2\sigma_I^2}\right) \exp\left(-\frac{\|X(i) - X(j)\|^2}{2\sigma_X^2}\right). \quad (5)$$

The graph H combines two grouping cues in a single weight.¹ Using the normalized cut criteria, pixels are encouraged to be grouped together if they have similar appearance and are close to each other. Note, however, that pixels that have similar appearance but are far away are not encouraged to be grouped because the corresponding weight is close to zero. Similarly, neighboring pixels that have very different appearance (such as in a textured region) are also not encouraged to be grouped.

3 New Criteria for Image Segmentation

We combine two normalized cut values to obtain a new criteria for image segmentation. We break the grouping cues (spatial proximity and appearance similarity) into two separate graphs, G_{grid} and G_{data} . Both graphs are defined over the same set of vertices, corresponding to the pixels in an image.

1. The graph G_{grid} is a grid over the image pixels, where each pixel is connected to the four neighboring pixels with an edge of weight 1. This graph encourages neighboring pixels to be grouped together, independent of their appearance.
2. The graph G_{data} is a fully connected graph that encourages pixels with similar appearance to be grouped together, independent of their location. The weights in G_{data} are based on appearance similarity of pixels, and do not depend on pixel locations,

$$w(i, j) = \exp\left(-\frac{\|I(i) - I(j)\|^2}{2\sigma^2}\right). \quad (6)$$

3.1 Spatial Information: G_{grid}

Let (A, B) be a cut in the grid graph. The cut defines a segmentation of the image into two regions, with a boundary Γ between them. The cut value, $\text{Cut}(A, B|G_{\text{grid}})$, counts the number of neighboring pixels that are in different regions. In general the cut value in the grid graph and similar graphs can be seen as a measure of the length of the boundary Γ (see [3]).

Observation 1.

$$\text{Cut}(A, B|G_{\text{grid}}) \approx \text{Len}(\Gamma).$$

This is a commonly used measure of spatial coherence in image segmentation problems (see, e.g., [4]). Although the criteria $\text{Cut}(A, B|G_{\text{grid}})$ leads to spatially coherent segmentations and is widely used in practice, it gives most preference to trivial solutions with a small (single pixel) region.

Using the previous observation and noting that $\text{Vol}(S|G_{\text{grid}}) \approx 4|S|$ we can derive an expression for the value of a normalized cut in the grid graph.

Observation 2.

$$\text{NCut}(A, B|G_{\text{grid}}) \approx \frac{|V| \text{Len}(\Gamma)}{4 |A||B|}.$$

Minimizing this criteria encourages solutions where the boundary Γ between the two regions is short (to minimize $\text{Len}(\Gamma)$) and where the two regions have similar size (to maximize $|A||B|$).

3.2 Global Appearance Information: G_{data}

Now we consider the weight of cuts and normalized cuts in G_{data} .

For $S \subseteq V$ we use g_S to denote a kernel density estimate defined by the pixel values in S ,

$$g_S(c) = \frac{1}{|S|} \sum_{i \in S} K(I(i) - c). \quad (7)$$

¹The graph defined here differs slightly from the one used in [1] because in [1] the weight of an edge is set to 0 if the distance between i and j is above a threshold.

Proposition 1.

$$\text{Cut}(A, B|G_{\text{data}}) = (2\pi\sigma^2)^{\frac{d}{2}}|A||B|\langle g_A, g_B \rangle,$$

where d is the dimension of the pixel appearance vectors, g_A and g_B are density estimates defined using a Gaussian kernel, and $\langle \cdot, \cdot \rangle$ denotes the standard inner product of functions.

Proof. We use the fact that the convolution of two Gaussians with equal variance is a Gaussian with twice the variance,

$$\begin{aligned} \sum_{i \in A, j \in B} w_{\text{data}}(i, j) &= \sum_{i \in A} \sum_{j \in B} \exp\left(-\frac{\|I(i) - I(j)\|^2}{2\sigma^2}\right) \\ &= (2\pi\sigma^2)^{\frac{d}{2}} \sum_{i \in A} \sum_{j \in B} \int_{-\infty}^{\infty} \left(\frac{1}{\pi\sigma^2}\right)^d \exp\left(-\frac{\|I(i) - c\|^2}{\sigma^2}\right) \exp\left(-\frac{\|I(j) - c\|^2}{\sigma^2}\right) dc \\ &= (2\pi\sigma^2)^{\frac{d}{2}} \int_{-\infty}^{\infty} \left(\sum_{i \in A} K_{\sigma^2}(I(i) - c)\right) \left(\sum_{j \in B} K_{\sigma^2}(I(j) - c)\right) dc \\ &= (2\pi\sigma^2)^{\frac{d}{2}}|A||B| \int_{-\infty}^{\infty} g_A(c)g_B(c)dc = (2\pi\sigma^2)^{\frac{d}{2}}|A||B|\langle g_A, g_B \rangle, \end{aligned} \quad (8)$$

Here $K_{\beta}(\cdot)$ is a Parzen window of bandwidth β . □

The proposition above is related to the Laplacian PDF Distance in [5]. It is also related to the work in [6] where a different graph construction is used to define global appearance models.

The weight of a cut in G_{data} will be minimized when the pixel values in the two regions have complementary support. Although this intuitively makes sense, the measure encourages regions to be unbalanced in size due to the term $|A||B|$ multiplying $\langle g_A, g_B \rangle$.

In order to derive an expression for $\text{NCut}(A, B|G_{\text{data}})$, we first use a similar reasoning as in the proposition above to note that $\text{Vol}(S|G_{\text{data}}) = (2\pi\sigma^2)^{(d/2)}|S||V|\langle g_S, g_V \rangle$. Then, from the definition of the normalized cut we obtain the following result.

Proposition 2.

$$\text{NCut}(A, B|G_{\text{data}}) = \langle g_V, g_V \rangle \frac{\langle g_A, g_B \rangle}{\langle g_A, g_V \rangle \langle g_B, g_V \rangle}.$$

This criteria is minimized when the distributions g_A and g_B have little overlap and both have significant overlap with g_V . In particular it penalizes solutions where one region does not represent a significant amount of the image data.

3.3 Combining Spatial and Appearance information

The normalized cut values in G_{grid} and G_{data} provide complementary measures for image segmentation. To combine the spatial and appearance cues we use a convex combination,

$$\text{MixNCut}(A, B) = (1 - \lambda) \text{NCut}(A, B|G_{\text{data}}) + \lambda \text{NCut}(A, B|G_{\text{grid}}). \quad (9)$$

The parameter $\lambda \in [0, 1]$ controls the relative importance of the two normalized cut measures.

We interpret $\text{MixNCut}(A, B)$ as a mixture of an appearance and a spatial term,

$$\text{MixNCut}(A, B) \approx (1 - \lambda) \left(\langle g_V, g_V \rangle \frac{\langle g_A, g_B \rangle}{\langle g_A, g_V \rangle \langle g_B, g_V \rangle} \right) + \lambda \left(\frac{|V| \text{Len}(\Gamma)}{4 |A||B|} \right). \quad (10)$$

The first term encourages a partition of the image into regions with dissimilar color distributions, while the second term encourages a spatially coherent partition. Both terms are normalized and avoid biases towards solutions with small regions. Note that each term is normalized in a particular way that is natural and has appropriated dimensions for the individual measures.

4 Segmentation Algorithm

4.1 Spectral Method

Let G_1 and G_2 be two weighted graphs. Now we describe a spectral method for optimizing a convex combination of two normalized cut values,

$$\text{MixNCut}(A, B|G_1, G_2) = (1 - \lambda) \text{NCut}(A, B|G_1) + \lambda \text{NCut}(A, B|G_2). \quad (11)$$

The approach is based on the Markov chain and conductance interpretation of normalized cuts ([1, 2]). Let W_1 and W_2 be the weighted adjacency matrices of the two graphs while D_1 and D_2 are the diagonal degree matrices. Let,

$$P_1 = D_1^{-1}W_1, \quad P_2 = D_2^{-1}W_2, \quad P = (1 - \lambda)P_1 + \lambda P_2. \quad (12)$$

The matrices P_1 and P_2 define two Markov chains on V . The matrix P also defines a Markov chain on V where in one step we follow P_1 with probability $(1 - \lambda)$ and P_2 with probability λ . We compute the second largest eigenvector of P to find a cut (A, B) with small conductance.

In our experiments, we use a Lanczos Process to compute the second largest eigenvector of P . We use k -means with $k = 2$ to cluster the entries in the eigenvector into 2 clusters.

4.2 Graph Sparsification

When the matrix P is sparse we can compute the required eigenvector much more quickly. The grid G_{grid} is sparse but G_{data} is dense. We sparsify the graph using a random sampling approach.

The approach described here is complementary to other methods that have been used to speed up the computation of eigenvectors for clustering. One such method is based on Nystrom approximation [7]. Another approach involves power iteration [8].

Let G be a weighted graph. To construct a sparse graph G' we independently sample m edges (with replacement) from G , with probabilities proportional to the edge weights. The weight of each sampled edge is set to 1 (adding up weights if there is repetition). With this approach the expected value of a cut (A, B) in G' equals the value of the cut in G up to a scaling factor of $(m / \text{Vol}(V|G))$. Moreover, if m is sufficiently large then with high probability every cut in G' has weight close to the cut value in G (up to a scaling factor of $(m / \text{Vol}(V|G))$) (see, e.g., [9]).

To implement this approach efficiently for G_{data} we need to sample edges with probability proportional to their weights $w(i, j)$ *without* enumerating all possible edges. We use an importance sampling method as a practical alternative.

First, partition V into L (≈ 1000 in practice) sets S_1, \dots, S_L with low appearance variance. We do this greedily, starting with a single set and repeatedly partitioning the set with highest variance into two using the k -means algorithm. Let m_i be the mean appearance of pixels in S_i and

$$q(a, b) = |S_a||S_b| \exp\left(-\frac{||m_a - m_b||^2}{2\sigma^2}\right). \quad (13)$$

To sample an edge for G' first select a random pair S_a and S_b with probability proportional to $q(a, b)$. Then select $i \in S_a$ and $j \in S_b$ uniformly at random. Finally, add the edge $\{i, j\}$ to G' with weight $w'(i, j) = |S_a||S_b|w(i, j)/q(a, b)$.

5 Numerical Experiments

For the experiments with MixNCut we use the graph sparsification method described above, where the number of sampled edges used to sparsify G_{data} was set to $m = 2|V|$.

We compare our new segmentation method with the original normalized cut formulation NCut using the graph H described in section 2.2. We sparsify this graph to scale the eigenvector computation to large images. Again, we accomplish this use an importance sampling approach.

Let H be the graph with weights defined by equation (5). To sample one edge from H , first select a pixel i uniformly at random. Then, draw a location x from a Normal distribution centered at $X(i)$

with variance σ_X^2 and select the pixel j closest to that location. We add the edge $\{i, j\}$ to G' with weight $w'(i, j) = \exp(-\|I(i) - I(j)\|^2 / 2\sigma_I^2)$. We repeat this process m times. In the following experiments we used $m = 100|V|$ to sparsify H .

5.1 Real Images

We tested our method on real images from a variety of datasets including the Berkeley Segmentation Dataset [10], the Plant Seedlings Dataset [11], the Grabcut dataset [12], the PASCAL VOC dataset [13] and a Scanning Electron Microscope (SEM) dataset [14]. Figure 2 shows some of the results we obtained, comparing the original normalized cuts formulation with our new approach. We can see in these examples how the new approach can segment challenging images in a variety of settings, often outperforming the original normalized cuts formulation.

Figure 3 illustrates segmentation results using MixNCut to partition an image into 3 regions. In this case we follow the approach suggested in [15] and [2], using k -means with $k = 3$ to cluster the pixels using the second and third largest eigenvector of the transition matrix P in equation (12).

For each example in these figures, we ran the algorithms using different parameter values (specified in the next section), and show the best result among the different runs.

5.2 Brodatz Textures

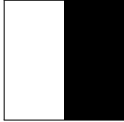
For a quantitative evaluation we used images with Brodatz textures [16]. To generate input images, we mixed pairs of textures using different ground-truth segmentation patterns and resized the result to 320×320 pixels. We compare MixNCut to NCut and a version of NCut with "texture features", where we use the magnitudes of the response of 12 Gabor filters (3 wavelengths and 4 orientations) to define appearance vectors for each pixel. Figure 4 shows some of the input images and segmentation results. The new MixNCut method defined directly in terms of "raw" pixel values finds near optimal segmentations in all of these examples, outperforming both baselines.

To measure the accuracy of a segmentation we use the Jaccard Index [17] $J(S, Q) = |S \cap Q| / |S \cup Q|$. Let (S, Q) be a ground-truth segmentation. We define the accuracy of a segmentation (A, B) as,

$$\text{Jaccard} = \max\left(\frac{J(S, A) + J(Q, B)}{2}, \frac{J(S, B) + J(Q, A)}{2}\right). \quad (14)$$

We use all pairings of the 10 textures in Figure 5 with three different ground-truth segmentations shown in Table 1 to generate three sets of images. We compute the mean accuracy of each method on each set of images using several parameter combinations ($\sigma_I \in \{20, 30, \dots, 100\}$ and $\sigma_X \in \{20, 30, \dots, 100\}$ for NCut; $\lambda \in \{.990, .995, .997\}$ and $\sigma \in \{.1, 1, 10, 30\}$ for MixNCut). Table 1 summarizes the best mean accuracy obtained with each method on each set of inputs. The table also shows the average running time of each method. We see the new MixNCut approach obtains near perfect accuracy (Jaccard ≈ 1) on all ground-truth patterns, significantly outperforming the other methods. The algorithms were implemented in MATLAB and run on a computer with an Intel i5-6200U CPU @ 2.30GHz using 8 GB of RAM running Linux.

Table 1: Evaluation of different segmentation methods on textured images. The table summarizes accuracy and running time of each method on images with different ground-truth segmentations.

									
	NCut	NCut + Gabor	MixNCut	NCut	NCut + Gabor	MixNCut	NCut	NCut + Gabor	MixNCut
Jaccard	0.91	0.94	0.96	0.57	0.77	0.93	0.55	0.70	0.92
Time (s)	10.37	12.78	9.09	10.91	12.95	6.61	10.37	14.12	7.15

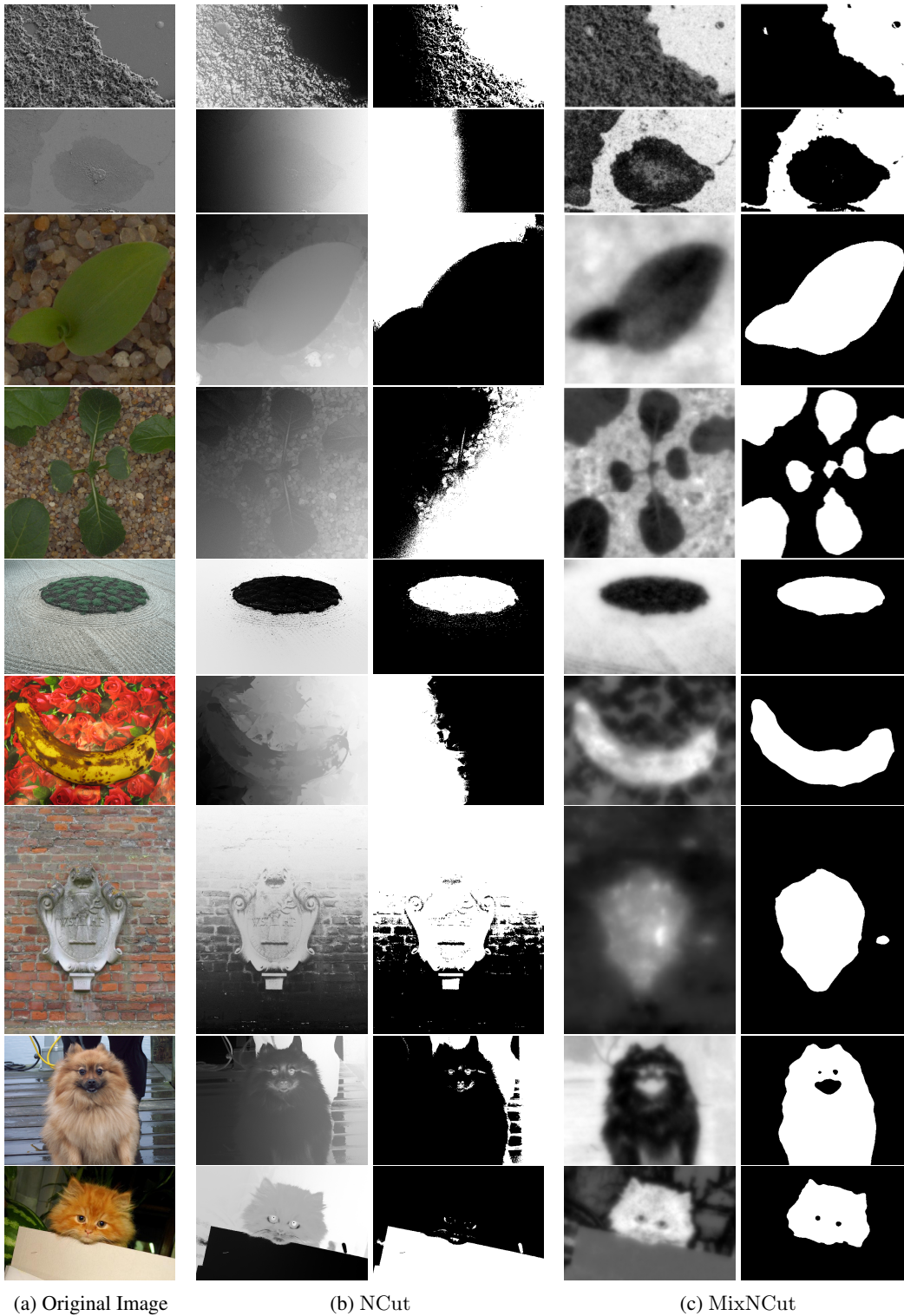


Figure 2: Segmentation results comparing Ncut and MixNcut on real images. Column (a) shows the input images. Column (b) shows the eigenvector found by the original Ncut formulation on the left and the segmentation result on the right. Column (c) shows the eigenvector found by the new MixNcut formulation on the left and the segmentation result on the right.

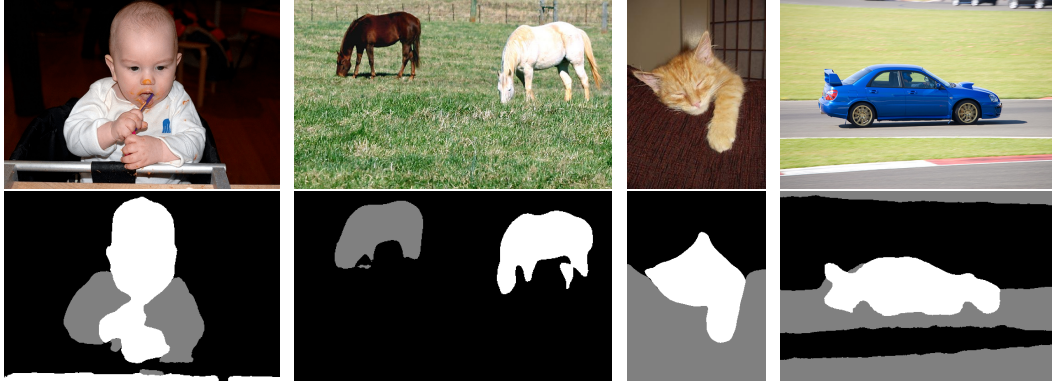


Figure 3: Segmentation results using the proposed method for images with more than 2 regions.

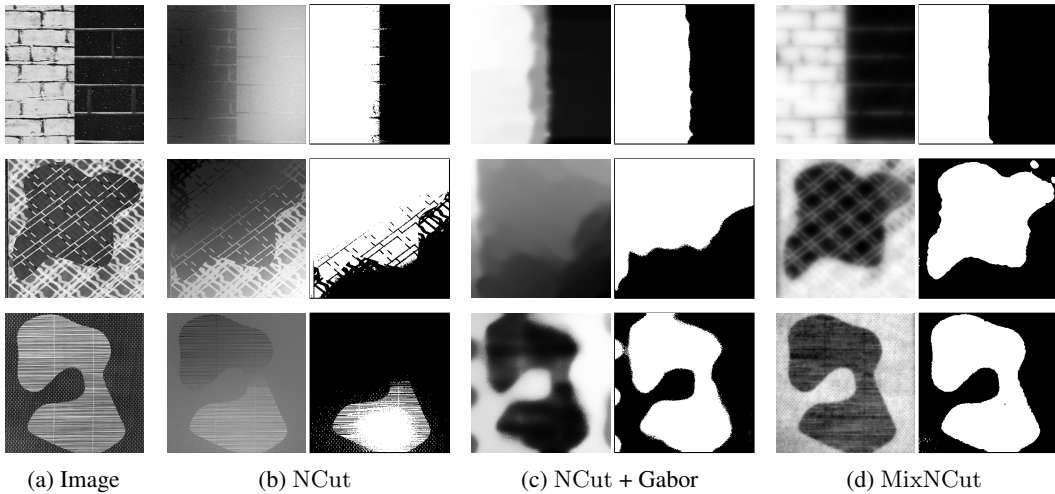


Figure 4: Comparing Ncut, Ncut + Gabor, and MixNcut on textured images. Column (a) shows the input images. Column (b) shows the eigenvector found by the original Ncut formulation on the left and the segmentation result on the right. Column (c) shows the eigenvector found by Ncut with Gabor features on the left and the segmentation result on the right. Column (d) shows the eigenvector found by the new MixNcut formulation on the left and the segmentation result on the right.

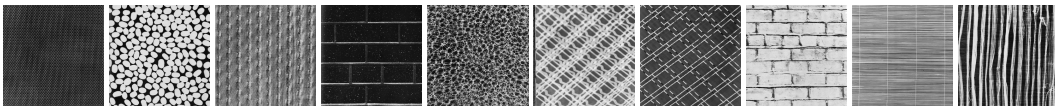


Figure 5: Brodatz Patterns used in the synthetic experiments

6 Conclusion

We introduced a new spectral method for image segmentation that can segment challenging images while working directly with "raw" pixel values, without any pre-processing or filtering. The approach is based on a novel combination of appearance and spatial grouping cues using two different graphs. We use a dense graph to capture appearance grouping cues. This leads to non-parametric models of region appearance. We also describe a technique that can be used to sparsify the resulting graph to ease the computational burden of spectral segmentation. Our results show that long range interactions can capture the appearance of complex regions and significantly improve the performance of graph-based segmentation methods. The proposed method is practical and it can be applied to different types of images (natural, biomedical, textures, etc.).

Broader Impact

Image segmentation has a variety of applications that can benefit all of society. For example, segmentation methods may enable advances in biomedical image analysis (including for medical diagnosis and treatment), tele-conferencing technology, human-computer-interaction, remote sensing, and robotics. However, there are also potential uses with questionable ethics, including mass surveillance and military applications.

References

- [1] Jianbo Shi and Jitendra Malik. Normalized cuts and image segmentation. *IEEE Transactions on Pattern Analysis and Machine Intelligence*, 22(8):888–905, 2000.
- [2] Marina Meila and Jianbo Shi. Learning segmentation by random walks. In *Advances in Neural Information Processing Systems*, pages 873–879, 2001.
- [3] Yuri Boykov and Vladimir Kolmogorov. Computing geodesics and minimal surfaces via graph cuts. In *IEEE International Conference on Computer Vision*, 2003.
- [4] David Mumford and Jayant Shah. Optimal approximations by piecewise smooth functions and associated variational problems. *Communications on pure and applied mathematics*, 42(5): 577–685, 1989.
- [5] Robert Jenssen, Deniz Erdogmus, Jose Principe, and Torbjorn Eltoft. The laplacian PDF distance: A cost function for clustering in a kernel feature space. In *Advances in Neural Information Processing Systems*, pages 625–632, 2005.
- [6] Meng Tang, Lena Gorelick, Olga Veksler, and Yuri Boykov. Grabcut in one cut. In *IEEE International Conference on Computer Vision*, pages 1769–1776, 2013.
- [7] Charless Fowlkes, Serge Belongie, Fan Chung, and Jitendra Malik. Spectral grouping using the nystrom method. *IEEE Transactions on Pattern Analysis and Machine Intelligence*, 26(2): 214–225, 2004.
- [8] Frank Lin and William W Cohen. Power iteration clustering. In *International Conference on Machine Learning*, 2010.
- [9] David P Williamson and David B Shmoys. *The design of approximation algorithms*. Cambridge University press, 2011.
- [10] D. Martin, C. Fowlkes, D. Tal, and J. Malik. A database of human segmented natural images and its application to evaluating segmentation algorithms and measuring ecological statistics. In *International Conference on Computer Vision*, volume 2, pages 416–423, July 2001.
- [11] Thomas Mosgaard Giselsson, Rasmus Nyholm Jørgensen, Peter Kryger Jensen, Mads Dyrmann, and Henrik Skov Midtby. A public image database for benchmark of plant seedling classification algorithms. *arXiv preprint arXiv:1711.05458*, 2017.
- [12] Carsten Rother, Vladimir Kolmogorov, and Andrew Blake. "Grabcut" interactive foreground extraction using iterated graph cuts. *ACM transactions on graphics (TOG)*, 23(3):309–314, 2004.
- [13] Mark Everingham, S.M. Ali Eslami, Luc Van Gool, Christopher K.I. Williams, John Winn, and Andrew Zisserman. The pascal visual object classes challenge: A retrospective. *International Journal of Computer Vision*, 111(1):98–136, 2015.
- [14] Rossella Aversa, Mohammad Hadi Modarres, Stefano Cozzini, and Regina Ciancio. NFFA-EUROPE - SEM dataset, 2018. URL <https://b2share.eudat.eu/records/80df8606fcdb4b2bae1656f0dc6db8ba>.
- [15] Andrew Y Ng, Michael I Jordan, and Yair Weiss. On spectral clustering: Analysis and an algorithm. In *Advances in Neural Information Processing Systems*, pages 849–856, 2002.

- [16] Phil Brodatz. *Textures: a photographic album for artists and designers*. Dover Pubns, 1966.
- [17] Paul Jaccard. Étude comparative de la distribution florale dans une portion des alpes et des jura. *Bull Soc Vaudoise Sci Nat*, 37:547–579, 1901.